Structure and Insight into Blue Light-Induced Changes in the BlrP1 BLUF Domain[†,‡]

Qiong Wu and Kevin H. Gardner*

Departments of Biochemistry and Pharmacology, University of Texas Southwestern Medical Center, 5323 Harry Hines Boulevard, Dallas, Texas 75390-8816

Received December 8, 2008; Revised Manuscript Received January 29, 2009

ABSTRACT: BLUF domains (sensors of blue light using flavin adenine dinucleotide) are a group of flavin-containing blue light photosensory domains from a variety of bacterial and algal proteins. While spectroscopic studies have indicated that these domains reorganize their interactions with an internally bound chromophore upon illumination, it remains unclear how these are converted into structural and functional changes. To address this, we have solved the solution structure of the BLUF domain from *Klebsiella pneumoniae* BlrP1, a light-activated *c*-di-guanosine 5′-monophosphate phosphodiesterase which consists of a sensory BLUF and a catalytic EAL (Glu-Ala-Leu) domain [Schmidt et. al. (2008) *J. Bacteriol. 187*, 4774–4781]. Our dark state structure of the sensory domain shows that it adopts a standard BLUF domain fold followed by two C-terminal α helices which adopt a novel orientation with respect to the rest of the domain. Comparison of NMR spectra acquired under dark and light conditions suggests that residues throughout the BlrP1 BLUF domain undergo significant light-induced chemical shift changes, including sites clustered on the $\beta_4\beta_5$ loop, β_5 strand, and $\alpha_3\alpha_4$ loop. Given that these changes were observed at several sites on the helical cap, over 15 Å from chromophore, our data suggest a long-range signal transduction process in BLUF domains.

Sensors of blue light using flavin adenine dinucleotide (FAD) (BLUF domains[1]) (*1*) are a recently discovered group of blue light photoreceptors distributed among a variety of proteins in bacteria and lower eukaryotes. These proteins detect light using FAD chromophores, undergoing a characteristic red 10 nm shift of their UV−visible absorption spectra after blue light illumination (*2*) to form a signaling state. Upon returning to dark conditions, the signaling conformation spontaneously decays to the ground-state with kinetics that varies from seconds to minutes (*3, 4*) in different proteins. The photoactivated conformations of these proteins demonstrate a variety of altered functional properties, including changes in protein−protein interactions and, ultimately, gene regulation (AppA) (*2, 5*), adenyl cyclase activity (PAC) (*6, 7*), and oligomerization state (PixD/PixE) (*8*). These data clearly indicate that this common input domain, triggered by a common stimulus, can be harnessed to regulate a wide range of biological activities within different protein contexts. However, the molecular mechanism of this control is still unclear and remains a topic of significant speculation.

To provide further data to this end, we have undertaken a series of biophysical studies of BlrP1 (blue light regulated phosphodiesterase 1) (*9*), a BLUF-containing protein from *Klebsiella pneumoniae*. This soluble, two-domain protein provides a good model for studying BLUF regulation of biological activity, as it avoids issues with unknown effectors (e.g., BlrB) or more complicated proteins (e.g., AppA, PAC). The domain architecture of BlrP1 (Figure 1a) shows an N-terminal photosensory BLUF domain followed by a phosphodiesterase EAL (Glu-Ala-Leu) domain. EAL domains regulate cellular levels of cyclic-di-guanosine 5′-monophosphate (GMP), a ubiquitous bacterial second messenger, via its destruction in opposition to GGDEF domain-containing diguanylate cyclases that catalyze its production (*10*−*13*). The presence of BLUF and EAL domains in BlrP1 implies that blue light should influence the activity of this enzyme, which has recently been demonstrated by a light-induced increase in phosphodiesterase activity (*14*). However, it remains unclear how light-induced structural changes originating in the BLUF domain are transmitted to the EAL domain and influence its catalytic activities. Previous studies on BLUF domains have implicated photochemically triggered alterations in the surrounding β-sheet and an accompanying C-terminal helical cap observed in most, but not all, BLUF structures as the possible interface to regulate the light-mediated signal between the BLUF domain core and its effectors (*8, 15, 16*).

To further test the generality of this sheet-and-cap model, we focused our attention on the BlrP1 BLUF domain (BlrP1 BLUF). We started by demonstrating that this domain is self-contained, bound a flavin chromophore, and was properly photocycled, but only when it contained a 50 residue C-terminal extension in addition to the canonical BLUF α/β core. Using solution NMR spectroscopy, we determined the dark state structure of BlrP1 BLUF, confirming that the

* To whom correspondence should be addressed. Phone: 1-214-645-6365. Fax: 1-214-645-6353. E-mail: kevin.gardner@utsouthwestern.edu.

† This work was supported by a grant from the Robert A. Welch Foundation (I-1424) to K.H.G.

‡ Coordinates have been deposited with the RCSB PDB (PDB ID 2KB2).

[1] Abbreviations: BLUF domain, sensor for blue light using FAD; BlrP1, blue light tegulated phosphodiesterase 1.

10.1021/bi802237r CCC: $40.75
Published on Web 02/03/2009

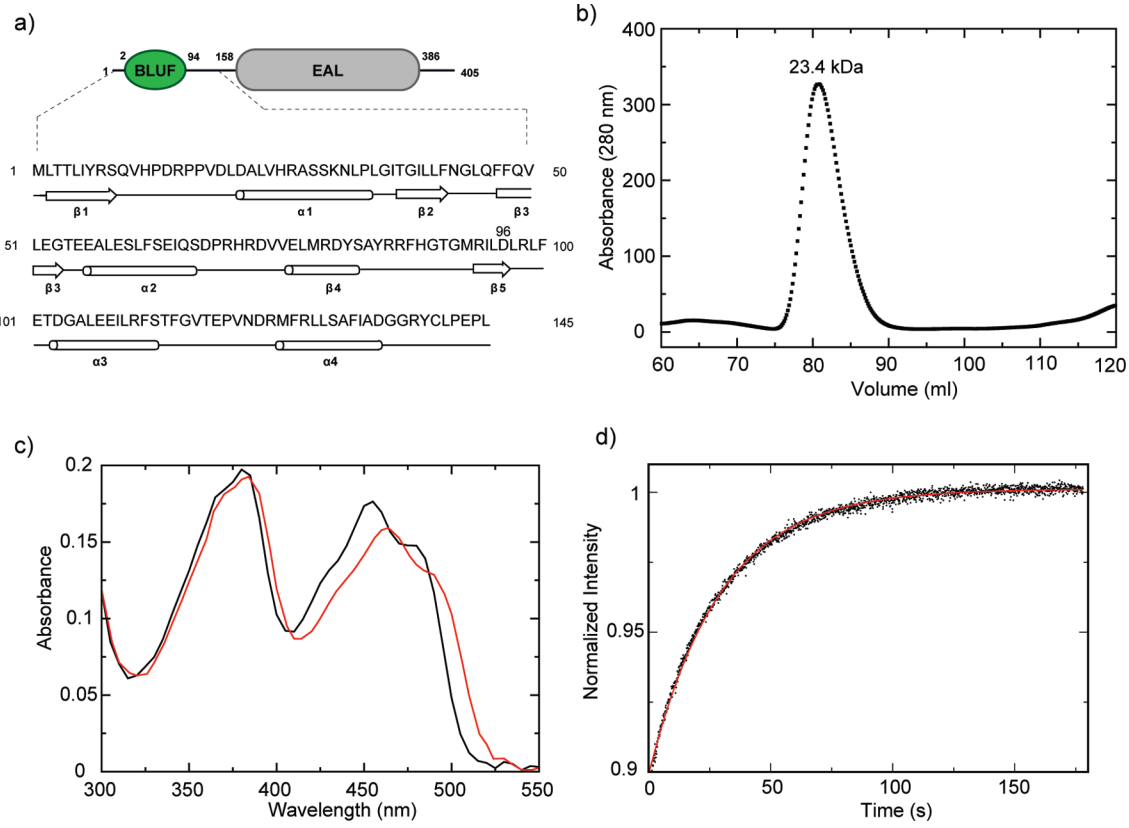

FIGURE 1: BlrP1 domain architecture and initial characterization of BlrP1 BLUF. a. Schematic representations of BlrP1 domain architecture and BLUF domain secondary structure. The domain boundaries were obtained from Hidden Markov model analyses of the BlrP1 sequence using the Pfam web service (*51*). The sequence of BLUF domain is provided with a ribbon representation of the secondary elements observed in solution structure. b. Gel filtration chromatography elution profile of BlrP1 BLUF. c. UV−visible absorbance spectra for the dark and light state of BlrP1 BLUF (black, dark; red, light). d. Dark state recovery of BlrP1 BLUF at 446 nm in 50 mM Tris (pH 7), 30 mM NaCl at 25 °C. Data were fit to a single exponential decay function using program xmgrace (*51*) with $\tau = 28.2$ s.

C-terminal extension adopted a helical conformation as anticipated. However, this helical cap packed against the BLUF core in a novel way compared to existing BLUF domain structures (*17*−*19*), suggesting some degree of plasticity among family members. Comparing NMR spectra acquired under dark and light conditions, we found that BlrP1 BLUF exhibited more significant light-dependent chemical shift changes than corresponding BLUF domains from BlrB (*15*) and AppA (*20*), particularly involving a cluster of residues on the $\beta_4\beta_5$ loop, β_5 strand, and $\alpha_3\alpha_4$ loop. Further, we observed remote light-induced chemical shift changes at several sites on the helical cap (over 15 Å from chromophore), consistent with long-range conformational changes. Finally, we examined the properties of BlrP1 BLUF point mutants, targeting residues implicated in flavin binding and this possible signal transduction pathway. We demonstrated that aliphatic residues on the β-sheet (I39 and L41) provided an important structural anchor between the BLUF core and the helical cap and that changes here perturb light-induced signaling. These observations support the proposed signaling pathway: FAD to β-sheet, then to the helical cap, and finally to the downstream effectors.

MATERIALS AND METHODS

Protein Expression and Purification. DNA fragment encoding for BlrP1 residues 1−96 and 1−145 were polymerase chain reaction amplified from the full length *blrP* sequence (*9*) and subcloned into the pHis-Gβ1-parallel expression vector (*21*). *Escherichia coli* BL21(DE3) cells transformed with this plasmid were grown in M9 media containing 1 g/L $^{15}NH_4Cl$ for U−^{15}N samples and supplemented with 3 g/L $^{13}C_6$-glucose for U−$^{15}N/^{13}C$ labeled samples. Cultures were grown at 37 °C until reaching $A_{600} \sim 0.7$ and then induced overnight at 20 °C by adding 0.5 mM isopropyl β-D-thiogalactoside (IPTG). Cells were harvested by centrifugation and the resulting pellets resuspended in 50 mM Tris (pH 8.0) and 100 mM NaCl buffer and lysed by extrusion. Lysates were clarified by centrifugation at 12 000*g* for 30 min. Supernatants were loaded into a Ni^{2+}-nitrilotriacetic acid (Ni^{2+}-NTA) column in the same buffer (supplemented with 25 mM imidazole to reduce nonspecific binding), allowing the rapid affinity purification of His-Gβ1 tagged BlrP1 BLUF by eluting with 250 mM imidazole in 50 mM Tris (pH 8.0), 100 mM NaCl, and 5 mM β-mercaptoethanol buffer. After exchanging the eluted proteins into 50 mM Tris (pH 7.0), 30 mM NaCl, and 5 mM β-mercaptoethanol buffer, the His-Gβ1 tag was cleaved by adding 1 mg His_6 tobacco etch virus (His_6-TEV) protease (*22*) per 30 mg of protein. The His-Gβ1 tag and His_6-TEV protease were removed from BlrP1 BLUF by passing over Ni^{2+}-NTA again. Purified proteins were concentrated to 50 μM for UV−visible absorbance spectroscopy experiments and either 100 μM (for dark vs light NMR experiments) or 600 μM (for chemical shift assignment and nuclear Overhauser effect spectrometry (NOESY) experiments) for solution NMR experiments.

UV−Visible Absorbance Spectroscopy. All UV−visible absorbance spectra were acquired using a Cary50 (Varian) spectrophotometer. Samples were photoactivated using a photographic flash. The subsequent recovery of the dark state form of the flavin cofactor was monitored by the changes in the absorbance at 446 nm after illumination, recording A_{446} every 1 s with an integration time of 0.1 s. Rates were determined by averaging the fit of four separate measurements to a single exponential decay. A circulating water bath was used for temperature control of the sample in a quartz cuvette. Experiments were conducted at 25 °C in 50 mM Tris (pH 7) and 30 mM NaCl in H_2O.

Site-Directed Mutagenesis. Point mutations of the BlrP1 BLUF domain were generated using QuickChange (Stratagene) from wild-type DNA and primers including the desired mutations (I39L, I39V, I39Y, L41T, L41V, L41Y, Q49N, Q49L, T90W, T90S, T90Y, T90A, M92V, M92I, F112Y, F112L, V117F, and V117L). All changes were verified by DNA sequencing. Transformation, protein induction, and purification were performed as described above for wild-type.

NMR Spectroscopy. All NMR experiments were performed at 25 °C on Varian Inova 500, 600, and 800 MHz spectrometers, using nmrPipe for data processing (*23*) and NMRview for analysis (*24*). Dark state backbone chemical shift assignments were obtained using standard 3D ^{15}N-edited triple resonance experiments including HNCACB, CBCA(CO)NH, and HNCO spectra (*25*). Sidechain chemical shifts were assigned from HCCH total correlation spectroscopy (HCCH-TOCSY), HC(CO)NH-TOCSY, and C(CO)NH-TOCSY data, complemented for aromatic ring assignments by HBCB(CGCD)HD (*26*) and aromatic ^{13}C/^{1}H heteronuclear single quantum coherence (HSQC) data from a uniformly ^{13}C-,^{15}N-labeled sample and 2D double-quantum-filtered correlation spectroscopy (DQF-COSY), TOCSY (τ_m = 30 ms), and NOESY (τ_m = 50 ms) spectra of an unlabeled sample in 99.9% D_2O. Simultaneous ^{15}N-, ^{13}C-edited NOESY (τ_m = 120 ms) data were used to facilitate the chemical shift assignment at all stages and to obtain distance restraints for structure calculation. Backbone dihedral angle restraints were obtained from TALOS analysis (*27*) of backbone ^{15}N, ^{13}C, and ^{1}H chemical shifts.

To obtain NMR spectra of photoexcited BlrP1 BLUF samples, we generated blue light from a 5 W Coherent Inova-90C argon laser running in single wavelength mode at 457 nm, directing the output from this laser into a quartz fiber optic inserted into the NMR sample (*21*). Power levels at the end of this fiber were 90 mW as measured before each experiment. ^{15}N/^{1}H and constant time ^{13}C/^{1}H HSQC spectra of the light state of BlrP1 BLUF were recorded by preceding each transient in the NMR experiment with a 300 ms laser pulse during the recycle delay (total 1060 ms delay).

As a result of its relatively rapid dark state recovery rate ($\tau \sim 28$ s at 25 °C) and significant optical density at 457 nm in both dark and light states, a substantial amount of light is needed to populate the BlrP1 BLUF photoproduct state. Unfortunately, photobleaching precludes the possibility of full chemical shift assignments of the BlrP1 BLUF light state using standard triple resonance methods. Thus, all the light state chemical shift assignments of BlrP1 BLUF were made by simply pairing the nearest crosspeaks in dark and light state spectra where such pairings were unambiguous in well-resolved portions of both spectra. This was possible for 47 of 137 backbone amides and 36 of 93 methyl groups.

Structure Calculation. Following the chemical shift assignment, we used ARIA2 (ambiguous restraints for iterative assignment) (*28*) to assign NOEs from ^{15}N-, ^{13}C-edited NOESY data in an automated manner. BlrP1 BLUF structures were determined with a mix of automated and manual assignment of NOESY spectra. Given our observations and others (*15*−*17, 19*) that the adenine ring of FAD is highly solvent-exposed and does not make significant contacts with the protein, we simply modeled the FAD chromophore as a flavin mononucleotide (FMN). FMN topology and parameter files were obtained from the HIC-Up database (*29*), and a single FMN molecule was placed in the starting coordinates 30 Å from the BlrP1 BLUF to avoid biasing the structure calculation. Backbone dihedral angle restraints were created from TALOS (*27*) analysis, using bounds set to two times the standard deviation of the TALOS predictions and enforcing a minimum of ±30°. Hydrogen bond restraints were established by examining the conformations of residues in regular secondary structure (as established by patterns of NOEs and TALOS-generated ϕ, ψ restraints) in initial structure ensembles and implementing H-bond restraints when HN−O=C distances and angles were consistent with H-bonding. Of 500 structures in the final iteration of the refinement, the 20 lowest energy structures were analyzed using routines in ARIA2 and PROCHECK (*30*). Coordinates of BlrP1 BLUF have been deposited in the Protein Data Bank under accession code 2KB2.

RESULTS

Solution Structure of BlrP1 BLUF. In our previous studies on BlrB, a 140 amino acid residue protein which contains only a canonical mixed α/β BLUF domain and a pair of C-terminal helices, we demonstrated that this C-terminal extension is essential for the structural integrity and proper photocycling of the domain (*15*). To test the generality of this finding for other BLUF domains, we generated two BlrP1 constructs at different lengths: BlrP1(1−96), which included only a BLUF domain, and BlrP1(1−145), which included the BLUF and approximately 50 C-terminal residues from the linker between the BLUF and the EAL domains. Consistent with our experiences with comparable constructs for BlrB (*15*), the shorter construct suffered poor expression and low yield, did not appear to bind FAD, and precipitated during purification. In contrast, the longer construct, eluted as an elongated stable monomer at an apparent molecular mass of 23.4 kDa (Figure 1b), showed a 10 nm characteristic red shift of BLUF domains in the UV−visible absorbance spectrum upon light illumination (Figure 1c) with exponential dark state recovery kinetics ($\tau \sim 28$ s) as monitored by the absorbance of the flavin chromophore at 446 nm (Figure 1d). Further, BlrP1(1−145) (hereafter referred to as BlrP1 BLUF) displayed a well-dispersed ^{15}N/^{1}H HSQC spectrum, was very stable in solution during the course of multiday 3D NMR experiments, and was generally better suited for in-depth structural and biophysical studies.

Using solution NMR spectroscopy, we determined the structure of BlrP1 using over 4000 geometric constraints, including interproton distances, dihedral angles, and hydrogen bonds (Table 1). All of these data are well-satisfied by

Table 1: Statistics for BlrP1 BLUF Solution Structure Determination

list of constraints	number of constraints
NOE distance restraints	4138
unambiguous	2720
ambiguous	1418
hydrogen bond restraints	77
dihedral angle (θ, ϕ) restraints from TALOS	168
Structure Analysis	
average number of NOE violations greater than 0.5 Å	0
average number of dihedral violations greater than 5°	0
geometric analysis of 2° structured residues	
rmsd to mean	0.15 ± 0.02 Å (backbone) 0.45 ± 0.06 Å (all heavy atoms)
Procheck	73.4% most favored region 24.0% allowed region 2.3% generally allowed region 0.4% disallowed region

the 20 lowest-energy structures, which form a high precision ensemble (backbone pairwise root-mean-square deviation (rmsd) of 0.15 ± 0.05 Å for ordered regions in residues 2−9, 21−34, 37−42, 47−70, 75−82, 92−96, 102−113, and 124−135) as shown in Figure 2a. The BLUF domain of BlrP1 has five β strands and four α helices ordered as $\beta_1\alpha_1\beta_2\beta_3\alpha_2\beta_4\beta_5\alpha_3\alpha_4$ which can be broken into two substructures: the BLUF core domain ($\beta_1\alpha_1\beta_2\beta_3\alpha_2\beta_4\beta_5$) and a C-terminal cap domain ($\alpha_3\alpha_4$). The isoalloxazine ring of FAD is sandwiched between α_1 and α_2 helices inside the BLUF domain, leaving the adenosine monophosphate moiety solvent-exposed and flexible (Figure 2). The BlrP1 BLUF domain surrounds the FAD isoalloxazine ring of BlrP1 BLUF with a set of conserved residues among BLUF domains, setting up hydrogen bonds involving Asn34 (to the FAD N3 position) and Gln52 (to the FAD O4 and the Tyr 10 Oη). Similar hydrogen bond networks were also observed in other BLUF domain proteins (*17, 19, 31, 32*). Notably, we did not observe any issue with intermediate exchange broadening of signals from residues in either the β_3 or the β_5 strands as observed with AppA (*20*) or BlrB (*15*), providing qualitative evidence for differences in the stability of the protein/flavin complex in the dark state among different BLUF domains.

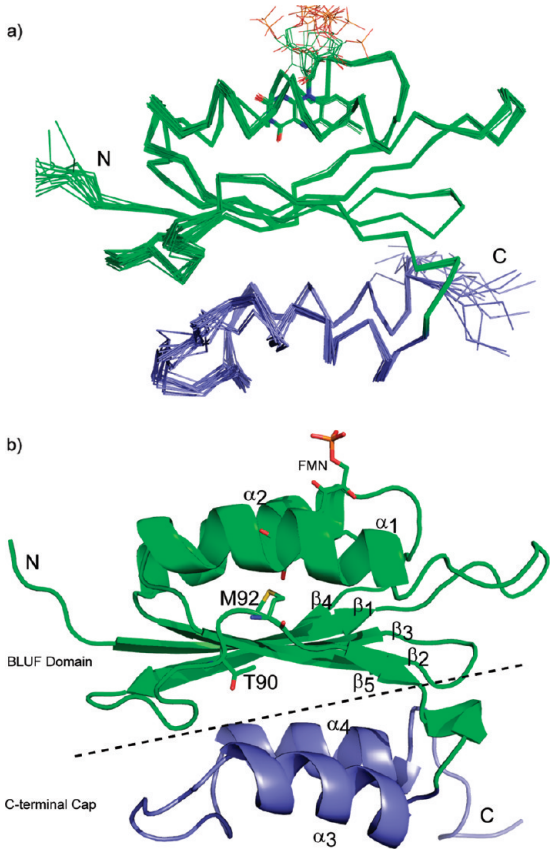

FIGURE 2: Solution structure of BlrP1 BLUF. a. Ensemble of the 20 lowest energy structures of BlrP1 BLUF, calculated as indicated in the text, with the FMN chromophore shown in stick representation. b. Ribbon diagram of the structure with the lowest energy in the ensemble shown in a. The canonical BLUF domain is colored green, and the C-terminal cap is colored blue. Secondary structure elements are as labeled.

While the structure of BLUF core of BlrP1 is similar to other BLUF domain structures, the last two α helices (α_3, α_4) adopt a rather different orientation (*17*−*20, 31, 33*). Compared to other BLUF domain structures, the BlrP1 BLUF helical cap is rotated ~90 degrees with respect to the central β strands, making the two cap helices almost parallel with, rather than perpendicular to, the β-sheet (Figure 2; Figure 1 of Supporting Information). The conserved residues T90 (W for most BLUF domains at that position) and M92 are located at the end of $\beta_4\beta_5$ loop with T90 pointing out and M92 pointing in the chromophore binding pocket, consistent with the orientations of the corresponding residues in most published BLUF structures (*17*−*19*). A notable exception for this is the AppA BLUF domain, which typically has the conserved tryptophan (W104) buried in the hydrophobic core near the chromophore-binding pocket (*20, 31, 32*).

Light-Induced Changes in BLUF Domain of BlrP1. To characterize the influence of blue light illumination on protein structure and dynamics of BlrP1 BLUF, we used solution NMR spectroscopy to investigate light-activated changes at the atomic level. Both dark and light NMR spectra of BlrP1 BLUF (Figure 3) were monitored at backbone amide and side chain methyl groups using $^{15}N/^{1}H$ and $^{13}C/^{1}H$ HSQC spectra, respectively. Unlike previous NMR studies of BLUF domains (e.g., BlrB (*15*), AppA (*20*)), crosspeaks in these spectra of BlrP1 BLUF display significant chemical shift changes after light excitation without widespread line broadening as seen for BlrB and AppA. This indicates that the BlrP1 BLUF light state has a different degree of conformational change or rates of conformational exchange than these other two BLUF domains, despite using the same photochemistry to initiate the changes. To systematically quantitate these light-activated chemical shift changes, we used minimum chemical shift difference analyses (*34*) on dark and light BlrP1 BLUF $^{15}N/^{1}H$ HSQC spectra. By this approach, peak locations from these spectra were compared to obtain the minimum chemical shift changes for each dark state peak to its nearest light state neighbor by the relationship $\Delta\delta_{mcs} = \min[((^{1}HN\ \Delta ppm)^2 + (0.17(^{15}N\ \Delta ppm)^2))^{1/2}]$ and plotted as a function of residue number (Figure 4a). This approach conservatively estimates the degree of chemical shift changes caused by illumination, even in spectral regions with significant chemical shift overlap. Not surprisingly, we observed relatively large light-activated chemical shift changes in the vicinity of the FAD chromophore (Figure 5a; Figure 3 of Supporting Information), on account of the

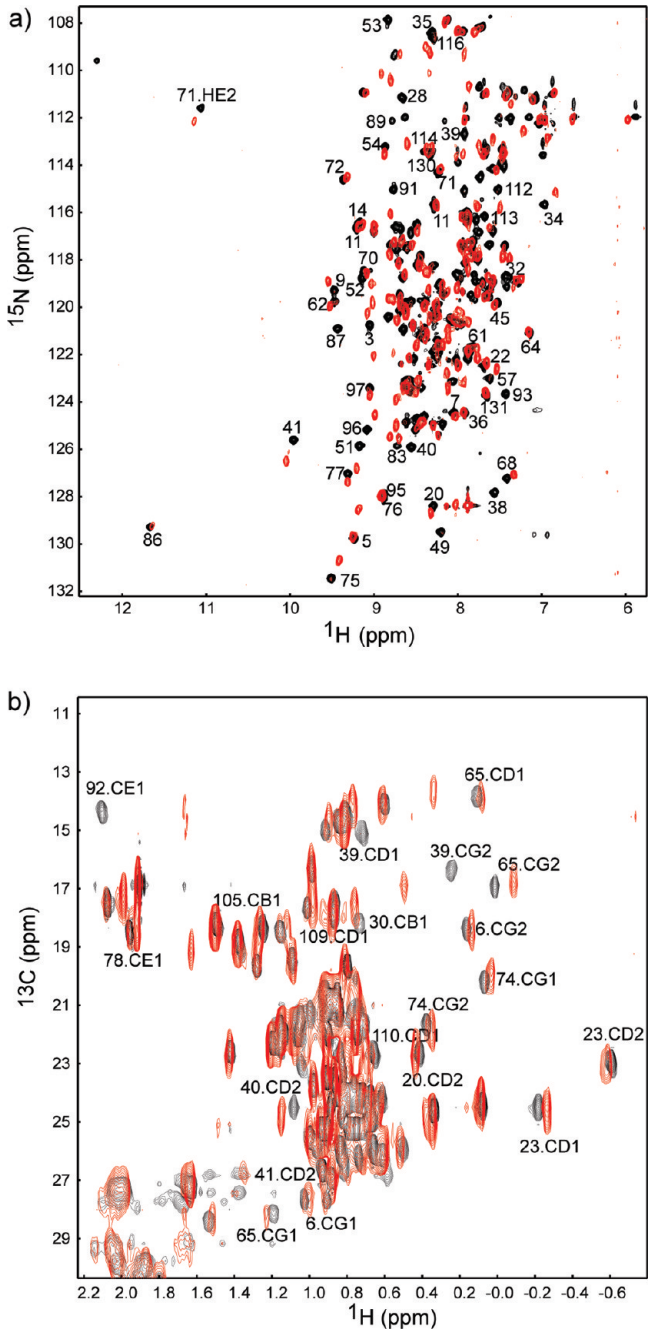

FIGURE 3: ^{15}N/^{1}H and ^{13}C/^{1}H HSQC spectra of BlrP1 BLUF under dark and light conditions. a. Dark (black) vs light (red) ^{15}N/^{1}H spectra of BlrP1 BLUF. b. Methyl region of dark (black) vs light (red) constant time ^{13}C/^{1}H HSQC spectra of BlrP1 BLUF. BlrP1 BLUF underwent significant chemical shift changes upon light illumination shown by both backbone ^{15}N/^{1}H and methyl side chain ^{13}C/^{1}H HSQC spectra. Sites with relatively large chemical shift changes are labeled with the assignments where available.

significant light-induced changes to the electronic structure of the isoalloxazine ring (*35*). However, we also noted that sites exhibiting above average light-induced minimum chemical shift changes clustered in a few interesting areas, specifically the β_4 and β_5 strands, the loop between them, and the loop between α_3 and α_4 (Figure 4b). More specifically, several sites (A105, I109, L110, F112, S113, G116, V117, and T118) over 15 Å from the chromophore displayed large light-induced chemical shift changes in both ^{15}N/^{1}H and ^{13}C/^{1}H HSQC spectra (Figure 5a; Figure 3 of Supporting Information), indicating that the light-activated signal around

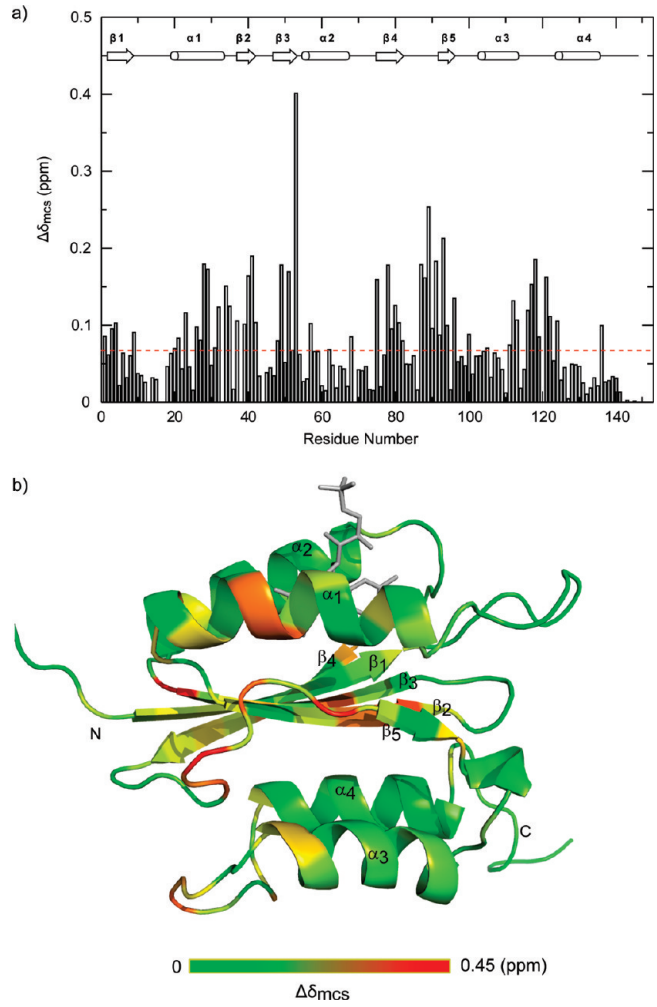

FIGURE 4: Minimum chemical shift difference analysis on dark and light states of BlrP1 BLUF. a. Minimum chemical shift differences from ^{15}N/^{1}H HSQC spectra obtained in the dark and light states for BlrP1 BLUF. Secondary structure elements are as shown on top of the figure. Red dashed line indicates the noise level (0.065 ppm). b. Minimum chemical shift differences between these two spectra are mapped onto the solution structure of BlrP1 BLUF with a color gradient encoding the magnitude of the shift change.

the chromophore somehow involves these sites, possibly by a specific signal transduction pathway, and then likely to the EAL domain. This is consistent with other studies suggesting that these regions probably play an important role in activating and transforming the light-induced signal in BLUF domains (*33, 36, 37*). More evidence along this line is the Cε methyl group of M92, which shows the biggest chemical shift change (>2 ppm) after light excitation, suggesting that light significantly alters the chemical environment at this site (*15*). Yuan et al. recently proposed the $\beta_4\beta_5$ loop and the C-terminal α helices as the interface for PixD oligomerization when its interaction partner PixE is present under dark conditions. Major conformational changes on the interface after light illumination result in the disassembly of the $PixD_{10}$−$PixE_5$ complex (*8*).

Of particular interest were residues at the β-sheet interface between the BLUF domain and the C-terminal cap, including several (I39/L40/L41) which showed light-induced chemical shift changes in both ^{15}N/^{1}H and ^{13}C/^{1}H HSQC spectra (Figure 5a; Figure 3 of Supporting Information). The methyl groups of I39 and L41 point to the opposite side of the β-sheet as the FAD chromophore and are in close contact

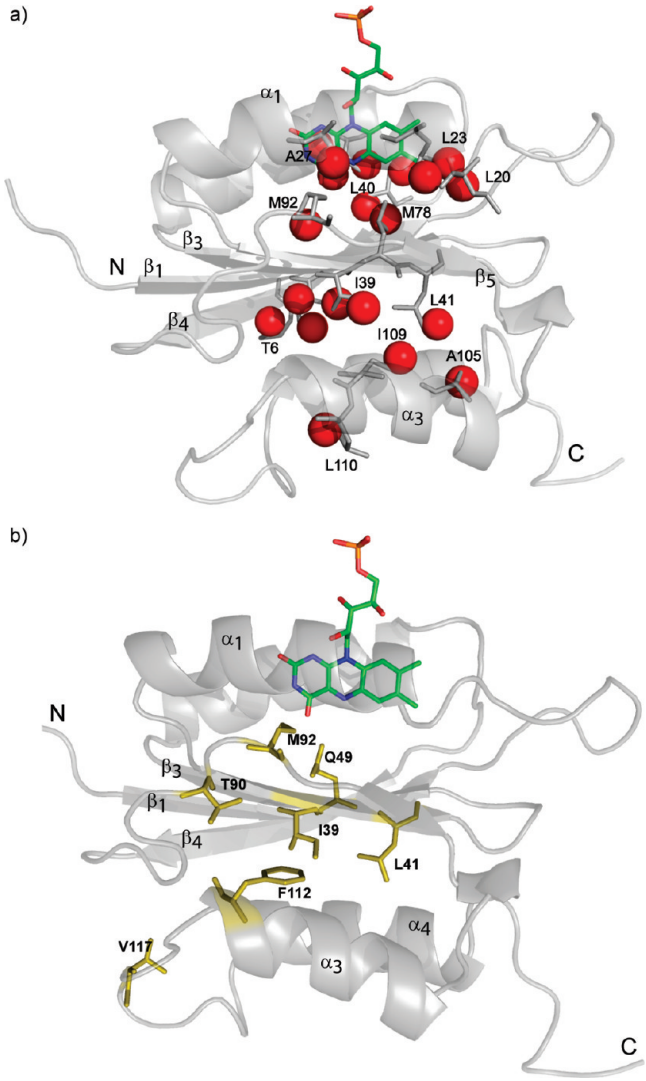

FIGURE 5: a. Light-perturbed sites in BlrP1 BLUF. Residues with light-dependent chemical shift change on methyl sites in $^{13}C/^{1}H$ dark versus light spectra are represented as sticks and labeled with residue numbers; the methyl sites are shown as red spheres. b. Mutated sites on BlrP1 BLUF. Mutated amino acid sites of BlrP1 BLUF on the structure: Ile39, Leu41, Gln49, Thr90, Met92, Phe112, and Val117. Sites are shown as gold sticks and labeled with residue numbers.

with the residues on the last two α helices as validated by strong NOE peaks between I39 and F112, I39 and L129, L41 and F132, and L41 and I133 in ^{13}C-edited NOESY spectra. These hydrophobic interactions appear to serve as an anchor between the sheet and the cap, locking the latter into the proper position and protecting the β-sheet from solvent exposure. On the basis of the destabilizing effects of deleting the helical cap from the BLUF domains of either BlrP1 or BlrB (*15*), we believe such protection is essential for many BLUF domains to maintain their structural and functional properties. In contrast, changes at L40 were expected given that it is located at the same side of FAD, ~3.5 Å away from the chromophore (and has NOE peaks with the FAD methyl C7a group). The fact that these three residues exhibit such significant and concerted light-dependent effects strongly supports the speculation that the light-activated signal may be passed from FAD to the β-sheet, then to the helical cap, and eventually to the downstream effectors by the interactions between these residues with the chromophore and with the C-terminal cap.

BlrP1 BLUF Mutants: BLUF Core, Q49, T90, and M92. Our BlrP1 BLUF structure and light-dependent changes suggested several important residues in its FAD binding, structural stability, and photocycling. To investigate these residues in more detail, we made a series of point mutants in the BLUF α/β core (Q49, T90, and M92), in the anchor coupling the core BLUF fold to the C-terminal helical cap (I39 and L41), and in the cap itself (F112 and V117) (Figure 5b; Figure 2 of Supporting Information). All of these residues are highly conserved, are critical for chromophore binding in other BLUF domains, or showed significant NMR chemical shift changes upon illumination. We evaluated the FAD-binding abilities and photochemical properties of these mutants using UV−visible absorbance spectroscopy (Table 1, Supporting Information), while we assayed their structural effects by comparing dark and light state $^{15}N/^{1}H$ HSQC spectra of the mutants with corresponding wild-type BlrP1 BLUF.

Our data indicate that two highly conserved residues in the BLUF core, Q49 and M92, are absolutely essential for FAD binding and photocycling. These sites were intolerant of any of the changes we made, as all mutants for these two residues completely abolished BlrP1 BLUF FAD binding capacity and corresponding photocycling, consistent with the results regarding their important roles in the structure and signaling of other BLUF domains (*15, 31, 33, 38*).

The third residue we selected for mutagenesis in the BLUF core was T90, which has been implicated in playing a central role in signal transduction mechanism together with M92 (*33, 39*). Notably, this β_5 strand position is highly conserved as a Trp residue in most BLUF domains (Figure 1, Supporting Information) but has been replaced with a Thr in BlrP1 BLUF and an Ala in the similar *E. coli* YcgF protein. All four T90 mutants that we examined still bound FAD and properly photocycled, albeit with ~1.1−2.5-fold slower dark state recovery rates compared with wild-type BlrP1 BLUF. These changes and corresponding differences in $^{15}N/^{1}H$ HSQC spectra were relatively subtle for T90A and T90S but were more dramatic for T90Y and T90W. Of particular interest is a comparison of dark versus light NMR spectra of T90W, which revealed that the light states of the wild-type and T90W BlrP1 BLUF exhibit somewhat different properties. Notably, the T90W light state spectrum shows significant line broadening in addition to the chemical shift changes observed for the wild-type protein (Figure 4, Supporting Information). Further, the newly generated indole $^{15}N\varepsilon/^{1}H\varepsilon$ crosspeak of T90W—which is unique in the $^{15}N/^{1}H$ HSQC spectrum, as the wild-type BlrP1 BLUF domain lacks any Trp residues—did not show any chemical shift change after light excitation (Figure 6c). These data strongly indicate that this indole ring does not undergo any light-driven transient exposure/burial, as has been speculated as a possible signaling mechanism for other BLUF domains (*33, 39*). While these data have been obtained on a BlrP1 BLUF point mutant, they are consistent with steady-state fluorescence results for the corresponding W104 of AppA in both wild-type and W64F backgrounds (*40*). Notably, the AppA W104 position is tolerant of point mutations even though the side chain is internally directed and near the FAD isoalloxazine ring (*41*). Masuda et al. observed similar results in PixD,

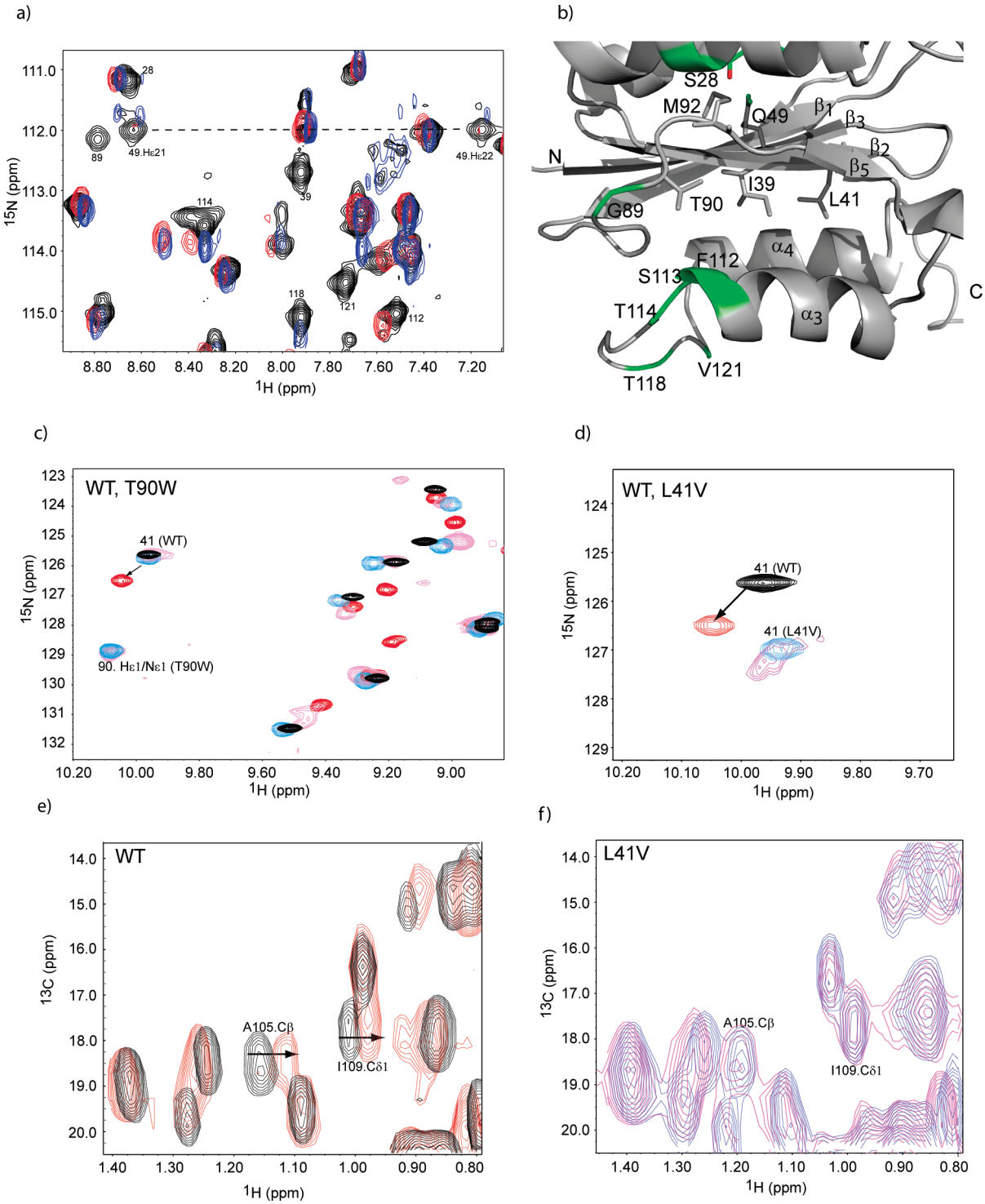

FIGURE 6: Light-dependent effect on the BlrP1 BLUF mutants. a. Overlay of ^{15}N/^{1}H HSQC spectra of BlrP1 BLUF mutants, residues with significant chemical shift changes in both of the mutants are as labeled. Wild-type (black), I39L (blue), and L41V (red). b. Sites showing consistent chemical shift changes in ^{15}N/^{1}H spectra for three mutants (L41V/I39L/I39V) are mapped on BlrP1 BLUF structure. These sites are F112, S113, T114, T118, and V121. c. Indole region of dark and light ^{15}N/^{1}H spectra of wild-type (black, red) and T90W mutant (cyan, pink) for BlrP1 BLUF. d. Residue 41 in dark and light ^{15}N/^{1}H HSQC spectra of wild-type (black, red) and L41V mutant (cyan, blue) of BlrP1 BLUF. e. Methyl groups of I109.Cδ1 and A105.Cβ in dark (black) and light (red) ^{13}C/^{1}H HSQC spectra of wild-type BlrP1 BLUF. f. Methyl groups of I109.Cδ1 and A105.Cβ in dark (cyan) and light (pink) ^{13}C/^{1}H HSQC spectra of BlrP1 BLUF L41V mutant.

finding that the M93A mutant of PixD (equivalent to BlrP1 M92) is light insensitive with biological activities incompatible with those of the light-adapted wild-type. However, W91A (T90 in BlrP1) retained light sensitivity and biological function (*38*). Putting these data together, it is clear that T90 is more tolerant of substitution, suggesting that it plays less of a role in domain stability and, potentially, signal transduction than other highly conserved residues.

BlrP1 BLUF Mutants: Anchor Between the BLUF Core and the Helical Cap, I39 and L41. As noted in our solution structure, I39 and L41 both project from the BLUF domain β-sheet toward the α_3/α_4 helical cap and show significant

light-induced chemical shift changes, suggesting that they may couple the BLUF core and helical cap structures together. Of the six mutations we generated at either I39 or L41, three (I39Y, L41Y, and L41T) lost the ability to bind FAD and precipitated during purification. The remaining three mutants (I39V, I39L, and L41V) all still bound FAD and exhibited the characteristic light-induced 10 nm red shift in their visible absorbance spectra. Supporting our findings that deletion of the helical caps destabilizes the BLUF core domains of BlrP1 BLUF (vide supra) and the BLUF-only protein BlrB (*15*), these data suggest that the specific packing of the BLUF β-sheet and the α helical cap is essential for FAD binding and domain stability.

Examination of the dark state $^{15}N/^{1}H$ HSQC spectra of I39V, I39L, and L41V mutants and the wild-type protein revealed that the point mutations induced chemical shift changes not only near the mutated residues but also at long distances involving residues in the helical cap. These long-range changes involved sites in the $\alpha_3\alpha_4$ loop (F112, S113, T114, T119, and V121) and the adjacent $\beta_4\beta_5$ loop (G89), with consistent chemical shift changes among all three mutants (I39L and L41V data shown in Figure 6a,b; I39V in Figure 5, Supporting Information). We speculate that the consistency of the observed chemical shift changes among the three mutants could reflect a cooperative movement of the helical cap in response to the different length of the mutated side chains.

Analogous comparisons of the effects of the I39V, I39L, and L41V mutations on light state $^{15}N/^{1}H$ spectra provided us with evidence that these sites might be involved in the transmission of conformational changes between the BLUF core and the helical cap. Notably, these mutations interfered with the interaction between the BLUF core and the helical cap as exhibited by smaller light-dependent chemical shift changes in the mutants. An example of this is provided by the backbone amide of V41, the mutated site in the L41V point mutant, which showed a greatly reduced light-induced chemical shift change in $^{15}N/^{1}H$ HSQC spectra and significant peak heterogeneity in the light state when compared to wild-type BlrP1 BLUF (Figure 6d). Notably, the light state $^{15}N/^{1}H$ HSQC spectra of all three mutants exhibited greater line broadening than we observed for the wild-type BlrP1 BLUF (Figure 6, Supporting Information), suggesting that these alterations perturbed the degree of conformational change (or exchange kinetics) associated with the light state.

We found similar effects in $^{13}C/^{1}H$ HSQC spectra, where the methyl groups of helical cap residues A105, I109, and L110 showed long-range light-dependent chemical shift changes for wild-type BlrP1 BLUF but much smaller effects for L41V (Figure 6e,f) where the dark and light state peaks are essentially overlapped. Unfortunately, resonances from L110 fall into a crowded region of the $^{13}C/^{1}H$ HSQC spectrum of L41V BlrP1 BLUF, complicating its assignment.

BlrP1 BLUF Mutants: Helical Cap, F112 and V117. Given that F112 and V117 are on the helical cap, far from the FAD chromophore, their light-dependent chemical shift changes strongly suggest that conformational changes are somehow propagated to these sites after illumination. To probe this effect, we made a total of four mutations (F112Y, F112L, V117L, and V117F) at these two sites. All four bound FAD, photocycled properly, and had similar dark regeneration rates as wild-type. While the light state $^{15}N/^{1}H$ spectra of these mutants generally shared similar patterns of light-induced chemical shift changes as wild-type, they also exhibit dramatic line broadening and accompanying reductions in peak intensities. Overall, substituting the two residues on the helical cap with other types of amino acids clearly did not interrupt the photochemistry and the interaction between chromophore and BlrP1 BLUF. However, the mutants display abnormal spectral behavior compared with wild-type protein in an amino acid type independent manner.

DISCUSSION

What defines a BLUF domain? Following the initial proposal of a conserved ~90 amino acid mixed α/β domain architecture from sequence homology (*1*), subsequent biophysical and biochemical studies have shown that this core BLUF domain is often associated with a helical C-terminal structural element (*17*−*19*). Truncation studies have further shown that these caps are essential for the stability of BLUF domains and FAD binding, demonstrating their necessity (*15, 16*). Extending this to a broader group of BLUF domains with secondary structure prediction (Figure 2, Supporting Information), we suggest that this is likely an integral element of many further BLUF domains, regardless of whether they originate from small proteins that consist solely of a BLUF domain ("BLUF-only proteins") or from larger proteins containing additional domains. This conservation implies a general role for the C-terminal helical cap, possibly protecting the β-sheet interface from solvent or facilitating a mechanism to propagate signals from the BLUF photosensory domain to the downstream effector.

Given this generality, it is interesting that the helical caps adopt different orientations with respect to the central β-sheet in different BLUF domains. This is best demonstrated with a structure-based superposition of five BLUF domain structures (*17*−*19, 31*) (Figure 1, Supporting Information) based on the conserved α/β secondary structure elements in the core. Notably, the helical caps of the three BLUF-only proteins are oriented almost perpendicular to the β-sheet, while BlrP1 BLUF (a component of a multidomain protein) has a helical cap that is almost parallel to the β-sheet. This is supported by a recently determined X-ray diffraction structure of full length BlrP1, the BLUF domain of which is very similar (1.1 Å Cα rmsd) to our structure (*14*), ruling out artifacts caused by either protein truncation or experimental approach. The different orientation of the helical cap may indicate a possible mechanism in regulating BLUF-containing proteins with otherwise very different biological functions.

Despite extensive structural and photochemical studies on BLUF domains (*15, 17*−*19, 31, 35*), their signaling mechanisms and its generality remains largely unknown. To date, it is widely accepted that a critical glutamine (Q49 in BlrP1) flips by 180° upon illumination, playing a central role in rearranging the protein/chromophore hydrogen-bonding network conserved among BLUF domains (*31, 35, 42*). In this study, our data support the important structural roles of several conserved residues Q49 and M92 in establishing the light-activated state as with other BLUF domains (*18*−*20, 31, 33*). However, the light state $^{15}N/^{1}H$ HSQC spectrum of BlrP1 BLUF is markedly different from those of other BLUF systems (e.g., AppA BLUF (*20*) and BlrB (*15*)) in that

photoactivation is accompanied by peak shifting rather than broadening. This is consistent with a greater degree of structural change or different kinetics of exchange across multiple protein conformations in the transient BlrP1 BLUF photoexcited states and also supports some diversity of signaling state structures and kinetics among BLUF domains (*43*). Although all BLUF domains display the same characteristic 10 nm red shift in the visible absorbance spectrum of the FAD chromophore upon illumination, the structural and kinetic properties of the subsequent conformational change may vary among BLUF domains. Here we observe that the $\beta_4\beta_5$ loop, β_5 strand, and $\alpha_3\alpha_4$ loop exhibit significant light-dependent conformational changes, consistent with observations from AppA BLUF (*20*), PixD (*19*), and BlrB (*15*). Further, residues T90 and M92 (in BlrP1 BLUF), which are the subject of intense debate regarding their roles in signal activation process for BLUF domains, are located on the β_5 strand (*33, 37, 39*) and show significant light-activated changes. Combining these observations and prior work raises the possibility that, after blue light illumination, the helical cap of BlrP1 BLUF undergoes some kind of reorientation process, and that might be associated with the conformational changes of the β_5 strand and the two loops.

Of particular interest on the β-sheet of BlrP1 BLUF are two methyl-containing residues, I39 and L41. These are both located in the β_2 strand, next to the β_5 strand in our solution structure. Our data clearly demonstrate that the side chains of these two residues are essential for the BLUF domain core to hold onto the helical cap and to maintain the FAD-binding capacity. Are they important in transmitting the light-induced signal as well? Limited evidence from the dark and light $^{13}C/^{1}H$ HSQC spectra of L41V shows that the light-induced chemical shift changes for residues A105 and I109 of wide-type do not exist in this mutant, suggesting that the mutation on this site interrupts the light-activated signal propagation in some way.

An interesting comparison is provided by another class of flavin-bound blue light photoreceptors, the LOV (Light-Oxygen-Voltage) domains. LOV and BLUF are both small flavin-based sensing units with similar, but not identical, α/β folds. Although both types of domains use similar chromophores (FMN versus FAD) to sense blue light, they rely on different photochemistries that are either solely noncovalent (BLUF domains) or result in the generation of new protein/flavin covalent bonds (LOV domains (*44*)). Intriguingly, LOV domains also utilize α helices outside the canonical domain boundaries, as shown with *Avena sativa* phototropin1 LOV2 (at both N- and C-termini) (*21, 45*) and *Neurospora crassa* Vivid (at N-terminus) (*46*). These helices cover the otherwise solvent-exposed β-sheet faces for both domains and are displaced or reoriented by light-induced conformational changes after illumination, analogously to the relationship between the BLUF domain and the cap regions. More broadly, the β-sheet interface appears to be important for a wide array of inter- and intramolecular interactions in varied biological systems that use the related PAS (Period-ARNT-singleminded) fold. These include the β-sheet interfaces of the HIF-2α and ARNT PAS-B domains that are used for PAS/PAS heterodimerization in the mammalian hypoxia response pathway (*47*−*49*) and the homodimeric β-sheet interface of the KinA PAS-A domain involved in *Bacillus subtilis* sporulation (*50*). Taken together, these data suggest that small sensor units may share interesting common features in signal sensing and transduction despite their differences in their sequence, structure, and functions.

ACKNOWLEDGMENT

We thank Ilme Schlichting and Mark Gomelsky for providing materials and information in advance of publication.

SUPPORTING INFORMATION AVAILABLE

Additional data and analyses in one table and six figures. This material is available free of charge via the Internet at http://pubs.acs.org.

REFERENCES

1. Gomelsky, M., and Klug, G. (2002) BLUF: A novel FAD-binding domain involved in sensory transduction in microorganisms. *Trends Biochem. Sci. 27*, 497–500.
2. Gomelsky, M., and Kaplan, S. (1998) AppA, a redox regulator of photosystem formation in Rhodobacter sphaeroides 2.4.1, is a flavoprotein. Identification of a novel FAD binding domain. *J. Biol. Chem. 273*, 35319–35325.
3. Kraft, B. J., Masuda, S., Kikuchi, J., Dragnea, V., Tollin, G., Zaleski, J. M., and Bauer, C. (2003) Spectroscopic and mutational analysis of the blue-light photoreceptor AppA: a novel photocycle involving flavin stacking with an aromatic amino acid. *Biochemistry 42*, 6726–6734.
4. Zirak, P., Penzkofer, A., Schiereis, T., Hegemann, P., Jung, A., and Schlichting, I. (2006) Photodynamics of the small BLUF protein BlrB from Rhodobacter sphaeroides. *J. Photochem. Photobiol., B 83*, 180–194.
5. Masuda, S., and Bauer, C. (2002) AppA is a blue light photoreceptor that antirepresses photosynthesis gene expression in *R. Sphaeroides*. *Cell (Cambridge, MA, U.S.) 110*, 613–623.
6. Iseki, M., Matsunaga, S., Murakami, A., Ohno, K., Shiga, K., Yoshida, K., Sugai, M., Takahashi, T., Hori, T., and Watanabe, M. (2002) A blue-light-activated adenylyl cyclase mediates photoavoidance in Euglena gracilis. *Nature 415*, 1047–1051.
7. Yoshikawa, S., Suzuki, T., Watanabe, M., and Iseki, M. (2005) Kinetic analysis of the activation of photoactivated adenylyl cyclase (PAC), a blue-light receptor for photomovements of Euglena. *Photochem. Photobiol. Sci. 4*, 727–731.
8. Yuan, H., and Bauer, C. E. (2008) PixE promotes dark oligomerization of the BLUF photoreceptor PixD. *Proc. Natl. Acad. Sci. U.S.A. 105*, 11715–11719.
9. Tyagi, A., Penzkofer, A., Griese, J., Schlichting, I., Kirienko, N. V., and Gomelsky, M. (2008) Photodynamics of blue-light-regulated phosphodiesterase BlrP1 protein from *Klebsiella pneumoniae* and its photoreceptor BLUF domain. *Chem. Phys. 354*, 130–141.
10. Christen, M., Christen, B., Folcher, M., Schauerte, A., and Jenal, U. (2005) Identification and characterization of a cyclic di-GMP-specific phosphodiesterase and its allosteric control by GTP. *J. Biol. Chem. 280*, 30829–30837.
11. Jenal, U., and Malone, J. (2006) Mechanisms of cyclic-di-GMP signaling in bacteria. *Annu. Rev. Genet. 40*, 385–407.
12. Paul, R., Weiser, S., Amiot, N. C., Chan, C., Schirmer, T., Giese, B., and Jenal, U. (2004) Cell cycle-dependent dynamic localization of a bacterial response regulator with a novel di-guanylate cyclase output domain. *Genes Dev. 18*, 715–727.
13. Schmidt, A. J., Ryjenkov, D. A., and Gomelsky, M. (2005) The ubiquitous protein domain EAL is a cyclic diguanylate-specific phosphodiesterase: enzymatically active and inactive EAL domains. *J. Bacteriol. 187*, 4774–4781.
14. Barends, T. R. M., Hartmann, E., Griese, J., Beitlich, T., Kirienko, N. V., Ryjenkov, D. A., Reinstein, J., Shoeman, R. L., Gomelsky, M., and Schlichting, I. (2009) Structure and mechanism of a bacterial light-regulated cyclic nucleotide phosphodiesterase, in press.
15. Wu, Q., Ko, W. H., and Gardner, K. H. (2008) Structural requirements for key residues and auxiliary portions of a BLUF domain. *Biochemistry 47*, 10271–10280.
16. Schreoder, C., Werner, K., Otten, H., Kratzig, S., Schwalbe, H., and Essen, L. (2008) Influence of a joining helix on the BLUF domain of the YcgF photoreceptor from Escherichia coli. *ChemBioChem 9*, 2463–2473.

17. Jung, A., Domratcheva, T., Tarutina, M., Wu, Q., Ko, W. H., Shoeman, R. L., Gomelsky, M., Gardner, K. H., and Schlichting, I. (2005) Structure of a bacterial BLUF photoreceptor: insights into blue light-mediated signal transduction. *Proc. Natl. Acad. Sci. U.S.A. 102*, 12350–12355.
18. Kita, A., Okajima, K., Morimoto, Y., Ikeuchi, M., and Miki, K. (2005) Structure of a cyanobacterial BLUF protein, Tll0078, containing a novel FAD-binding blue light sensor domain. *J. Mol. Biol. 349*, 1–9.
19. Yuan, H., Anderson, S., Masuda, S., Dragnea, V., Moffat, K., and Bauer, C. (2006) Crystal structures of the Synechocystis photoreceptor Slr1694 reveal distinct structural states related to signaling. *Biochemistry 45*, 12687–12694.
20. Grinstead, J. S., Hsu, S. T., Laan, W., Bonvin, A. M., Hellingwerf, K. J., Boelens, R., and Kaptein, R. (2006) The solution structure of the AppA BLUF domain: Insight into the mechanism of light-induced signaling. *ChemBioChem 7*, 187–193.
21. Harper, S. M., Neil, L. C., and Gardner, K. H. (2003) Structural basis of a phototropin light switch. *Science 301*, 1541–1544.
22. Blommel, P. G., and Fox, B. G. (2007) A combined approach to improving large-scale production of tobacco etch virus protease. *Protein Expression Purif. 55*, 53–68.
23. Delaglio, F., Grzesiek, S., Vuister, G. W., Zhu, G., Pfeifer, J., and Bax, A. (1995) NMRPipe: a multidimensional spectral processing system based on UNIX pipes. *J. Biomol. NMR 6*, 277–293.
24. Johnson, B. A. (2004) Using NMRView to visualize and analyze the NMR spectra of macromolecules. *Methods Mol. Biol. (Totowa, NJ, U.S.) 278*, 313–352.
25. Sattler, M., Schleucher, J., and Griesinger, C. (1999) Heteronuclear multidimentional NMR experiments for the structure determination of proteins in solution employing pulsed field gradients. *Prog. Nucl. Magn. Reson. Spectrosc. 34*, 93–158.
26. Yamazaki, T., Forman-Kay, J. D., and Kay, L. E. (1993) Two-dimensional NMR experiments for correlating carbon-13 β and proton δ/ε chemical shifts of aromatic residues in 13C-labeled proteins via scalar couplings. *J. Am. Chem. Soc. 115*, 11054–11055.
27. Cornilescu, G., Delaglio, F., and Bax, A. (1999) Protein backbone angle restraints from searching a database for chemical shift and sequence homology. *J. Biomol. NMR 13*, 289–302.
28. Linge, J. P., O'Donoghue, S. I., and Nilges, M. (2001) Antomated assignment of ambiguous nuclear overhauser effects with ARIA. *Methods Enzymol. 339*, 71–90.
29. Kleywegt, G. J. (2007) Crystallographic refinement of ligand complexes. *Acta Crystallogr., Sect. D 63*, 94–100.
30. Morris, A. L., MacArthur, M. W., Hutchinson, F. G., and Thornton, J. M. (1992) Stereochemical quality of protein structure corrdinates. *Protein Expression Purif. 12*, 345–365.
31. Anderson, S., Dragnea, V., Masuda, S., Ybe, J., Moffat, K., and Bauer, C. (2005) Structure of a novel photoreceptor, the BLUF domain of AppA from Rhodobacter sphaeroides. *Biochemistry 44*, 7998–8005.
32. Grinstead, J. S., Avila-Perez, M., Hellingwerf, K. J., Boelens, R., and Kaptein, R. (2006) Light-induced flipping of a conserved glutamine sidechain and its orientation in the AppA BLUF domain. *J. Am. Chem. Soc. 128*, 15066–15067.
33. Jung, A., Reinstein, J., Domratcheva, T., Shoeman, R. L., and Schlichting, I. (2006) Crystal structures of the AppA BLUF domain photoreceptor provide insights into blue light-mediated signal transduction. *J. Mol. Biol. 362*, 717–732.
34. Farmer, B. T., Constantine, K. L., Goldfarb, V., Friedrichs, M. S., Wittekind, M., Yanchunas, J., Jr., Robertson, J. G., and Mueller, L. (1996) Localizing the NADP+ binding site on the MurB enzyme by NMR. *Nat. Struct. Biol. 3*, 995–997.
35. Gauden, M., van Stokkum, I. H., Key, J. M., Luhrs, D. C., van Grondelle, R., Hegemann, P., and Kennis, J. T. (2006) Hydrogen-bond switching through a radical pair mechanism in a flavin-binding photoreceptor. *Proc. Natl. Acad. Sci. U.S.A. 103*, 10895–10900.
36. Masuda, S., Hasegawa, K., Ishii, A., and Ono, T. A. (2004) Light-induced structural changes in a putative blue-light receptor with a novel FAD binding fold sensor of blue-light using FAD (BLUF); Slr1694 of synechocystis sp. PCC6803. *Biochemistry 43*, 5304–5313.
37. Masuda, S., Tomida, Y., Ohta, H., and Takamiya, K. (2007) The critical role of a hydrogen bond between Gln63 and Trp104 in the blue-light sensing BLUF domain that controls AppA activity. *J. Mol. Biol. 368*, 1223–1230.
38. Masuda, S., Hasegawa, K., Ohta, H., and Ono, T. (2008) Crucial role in light signal transduction for the conserved Met93 of the BLUF protein PixD/Slr1694. *Plant Cell Physiol. 49*, 1600–1609.
39. Masuda, S., Hasegawa, K., and Ono, T. A. (2005) Tryptophan at position 104 is involved in transforming light signal into changes of beta-sheet structure for the signaling state in the BLUF domain of AppA. *Plant Cell Physiol. 46*, 1894–1901.
40. Toh, K. C., van Stokkum, I. H., Hendriks, J., Alexandre, M. T., Arents, J. C., Perez, M. A., van Grondelle, R., Hellingwerf, K. J., and Kennis, J. T. (2008) On the signaling mechanism and the absence of photoreversibility in the AppA BLUF domain. *Biophys. J. 95*, 312–321.
41. Gauden, M., Grinstead, J. S., Laan, W., van Stokkum, I. H., Avila-Perez, M., Toh, K. C., Boelens, R., Kaptein, R., van Grondelle, R., Hellingwerf, K. J., and Kennis, J. T. (2007) On the role of aromatic side chains in the photoactivation of BLUF domains. *Biochemistry 46*, 7405–7415.
42. Unno, M., Masuda, S., Ono, T. A., and Yamauchi, S. (2006) Orientation of a key glutamine residue in the BLUF domain from AppA revealed by mutagenesis, spectroscopy, and quantum chemical calculations. *J. Am. Chem. Soc. 128*, 5638–5639.
43. Bonetti, C., Mathes, T., van Stokkum, I. H., Mullen, K. M., Groot, M. L., van Grondelle, R., Hegemann, P., and Kennis, J. T. (2008) Hydrogen bond switching among flavin and amino acid side chains in the BLUF photoreceptor observed by ultrafast infrared spectroscopy. *Biophys. J. 95*, 4790–4802.
44. Salomon, M., Christie, J. M., Knieb, E., Lempert, U., and Briggs, W. R. (2000) Photochemical and mutational analysis of the FMN-binding domains of the plant blue light receptor, phototropin. *Biochemistry 39*, 9401–9410.
45. Halavaty, A. S., and Moffat, K. (2007) N- and C-terminal flanking regions modulate light-induced signal transduction in the LOV2 domain of the blue light sensor phototropin 1 from Avena sativa. *Biochemistry 46*, 14001–14009.
46. Zoltowski, B. D., Schwerdtfeger, C., Widom, J., Loros, J. J., Bilwes, A. M., Dunlap, J. C., and Crane, B. R. (2007) Conformational switching in the fungal light sensor Vivid. *Science 316*, 1054–1057.
47. Erbel, P. J., Card, P. B., Karakuzu, O., Bruick, R. K., and Gardner, K. H. (2003) Structural basis for PAS domain heterodimerization in the basic helix--loop--helix-PAS transcription factor hypoxia-inducible factor. *Proc. Natl. Acad. Sci. U.S.A. 100*, 15504–15509.
48. Scheuermann, T. H., Tomchick, D. R., Machius, M., Guo, Y., Bruick, R. K., and Gardner, K. H. (2009) Artificial ligand binding within the HIF2 alpha PAS-B domain of the HIF2 transcription factor. *Proc. Natl. Acad. Sci. U.S.A. 106*, 450–455.
49. Yang, J., Zhang, L., Erbel, P. J., Gardner, K. H., Ding, K., Garcia, J. A., and Bruick, R. K. (2005) Functions of the Per/ARNT/Sim domains of the hypoxia-inducible factor. *J. Biol. Chem. 280*, 36047–36054.
50. Lee, J., Tomchick, D. R., Brautigam, C. A., Machius, M., Kort, R., Hellingwerf, K. J., and Gardner, K. H. (2008) Changes at the KinA PAS-A dimerization interface influence histidine kinase function. *Biochemistry 47*, 4051–4064.
51. http://plasma-gate.weizmann.ac.il/Grace/ (accessed Jan 1, 2008).

BI802237R